

# High-Resolution Spectropolarimetry at the Italian Telescopio Nazionale Galileo

Francesco Leone<sup>a</sup>, Pietro Bruno<sup>a</sup>, Antonio Calí<sup>a</sup>, Riccardo Claudi<sup>b</sup>,  
Rosario Cosentino<sup>a</sup>, Giovanni Gentile<sup>a</sup>, Raffaele Gratton<sup>b</sup>, Salvatore Scuderi<sup>a</sup>

<sup>a</sup>INAF - Osservatorio Astrofisico di Catania, Via S. Sofia 78, I-95123 Catania, Italy

<sup>b</sup>INAF - Osservatorio Astronomico di Padova, Vicolo Osservatorio 5, I-35122 Padova, Italy

## ABSTRACT

The polarimeter built for the high resolution spectrograph (SARG) of the alto-azimuthal Telescopio Nazionale Galileo is presented.

This double-beam instrument, able to take into account time independent (instrumental) and time dependent (sky transparency) sensitivity, is based on a Fresnel prism ( $\lambda/2$ ) and K-prism ( $\lambda/4$ ) which gives an almost constant retard along the very large wavelength interval covered with new spectrographs: SARG covers the 370 - 1020 nm range and more than 300 nm in a single exposure.

The two flat metallic mirrors, which are necessary to feed the spectrograph, and the alto-azimuthal mounting of the telescope are responsible of an instrumental polarisation depending on the sky position of the target. A modelling of the instrumental polarisation and a hardware correction of the sky rotation are performed to measure the polarisation across stellar-like object at  $R = 115,000$  resolution.

**Keywords:** Polarimetry, Spectropolarimetry, High Resolution

## 1. INTRODUCTION

Observational astronomy mainly relates to the direction and intensity of electromagnetic radiation as a function of wavelength and time. However, electromagnetic radiation presents a further, even if commonly ignored, property that can be fundamental to understand the physics of the emitting region: the polarisation state.

Mechanisms responsible for polarised light from astronomical objects are:

- reflection from solid surface (planets),
- scattering by small grains, molecules and free electrons,
- Hanle and Zeeman effects.

Furthermore, polarised light can be also associated to radio emission.

Even if methods to measure the light polarisation degree of astronomical objects are well known from long time, this observational technique has not been very popular, we believe, mainly for two reasons: the very low level of the polarisation, that makes measurements very difficult (often even challenging), and the great difficulty in the theoretic interpretation of the results. The recent development of large telescope and instruments able to give very high signal-to-noise observations, together with the diffusion of high performance multi-processors computers have given a strong impulse to polarimetry.

Usually, spectropolarimetry is possible at low resolution, with the aim to observe the polarisation properties of the flux distribution of stellar or extra-galactic sources. Among the most recent examples: Schmid et al.<sup>12</sup> that observed the Seyfert 1 galaxy Fairall 51 at spectral resolution of  $\Delta\lambda \sim 4.5\text{\AA}$ , and Kawabata et al.<sup>11</sup> who

---

Further author information: (Send correspondence to F. Leone)

E-mail: fleone@ct.astro.it, Telephone: +39 095 7332-229

performed spectropolarimetry of the fast nova V1494 Aquilae at spectral resolution  $\Delta\lambda \sim 150\text{\AA}$ . Interest has been also devoted to relatively high resolution to measure the polarisation across wide spectral lines, as an example Harries & Howarth<sup>9</sup> measured (0.79 Å/px) the linear polarisation within the Raman lines for a sample of symbiotic stars.

Spectropolarimetry across stellar metal lines has been firstly performed from Babcock<sup>1</sup> who measured the magnetic field of *78 Virginis* from the wavelength distance of circular polarised  $\sigma$  components due to the Zeeman splitting. In conformity with the historically period, these observations were performed (at the best) with a linear dispersion only of 2.2 Å/mm but started a new aspect of the observational astronomy. In spite of that, no polarimeter unit has been dedicated to a high resolution spectrograph. At our knowledge, the polarimeters dedicated to the MuSiCoS échelle spectrograph and AAT-RGO spectrographs give the actually highest possible resolution ( $R \sim 35\,000$ ) spectropolarimetry.

Here, we discuss the importance of the high resolution spectropolarimetry and than we present the polarisation analyser that has been designed for the high resolution spectrograph (SARG) of the Italian *Telescopio Nazionale Galileo*. This polarimeter has been designed in order to properly work within the very large spectral range covered by the spectrograph and don't waste its very high efficiency.

This polarimeter has been designed and built at the *Osservatorio Astrofisico di Catania* in 2000 with *Consorzio Nazionale per l'Astronomia e l'Astrofisica* funds.

## 2. THE IMPORTANCE OF HIGH RESOLUTION SPECTROPOLARIMETRY

Solanki & Stenflo<sup>13</sup> studied the effects of spectral resolution on the measurement of the circular polarisation across line profiles. These authors showed that the area and amplitude of Stokes' V strongly decrease with increased spectral smearing.

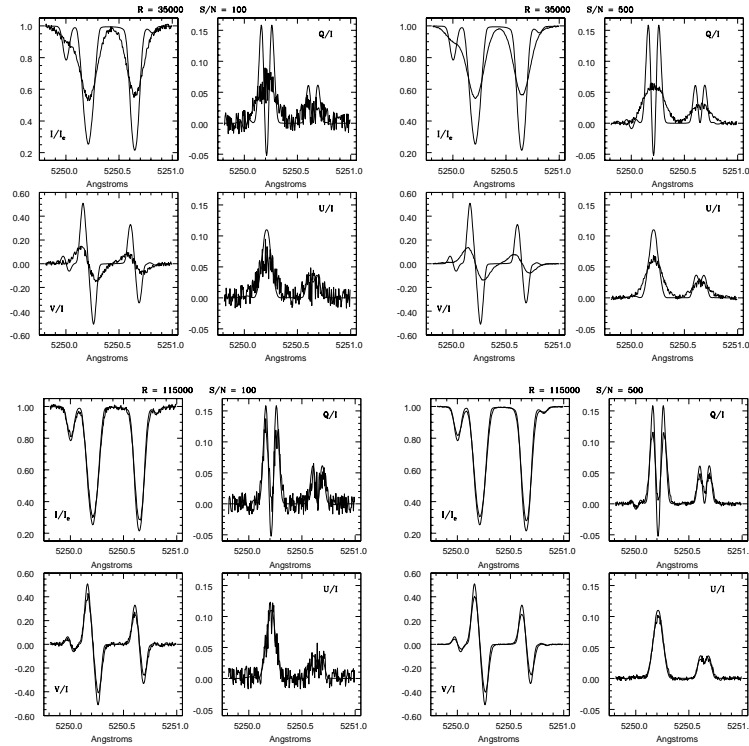
To point out the importance of high resolution in measuring the polarisation degree across spectral lines, we have solved the radiative transfer equation for the solar atmosphere model within a 1.5 Å interval centered at 5250.4 Å. In solving the radiative equation transfer we have assumed an uniform 1 KG magnetic field tilted with respect to the observer line of sight and clockwise rotated of 45° with respect to the equatorial reference system. We have also assumed a 2 km s<sup>-1</sup> rotational velocity.

Fig.1 shows computed Stokes parameters convolved with Gaussian profiles representing two different instrumental smearings. We note that for small resolving powers ( $R = 35\,000$ ) even at very high signal-to-noise ratio ( $S/N = 500$ ) it is not possible to recover the intrinsic structure of Stokes parameters. Differently, at higher resolving powers ( $R = 115\,000$ ) and relatively small  $S/N (= 100)$  the intrinsic Stokes parameters are reasonable recovered and that for  $S/N = 500$  these are perfectly defined.

## 3. TNG AND SARG

The Italian *Telescopio Nazionale Galileo* (TNG) is an alto-azimuthal telescope with a 3.55 m diameter and the Nasmyth foci only. It is located on the Roque de los Muchachos, La Palma, Canary Islands, Spain (Bortoletto et al.<sup>2</sup>

The SARG (Gratton et al.<sup>8</sup>) is a cross dispersed echelle spectrograph working in the 370 - 1020 nm wavelength range. By means of *blue, green, yellow* and *red* grisms it covers the 369-518, 419-567, 462-795 and 502-1020 nm wavelength intervals with one exposure respectively. The spectral resolution for slit width of 1 arcsec is  $R=46\,000$ . The maximum resolution is  $R=164\,000$  The spectrograph is rigidly connected to the TNG fork under the elevation axis of the telescope (Nasmyth B). The light feeding is provided by an optical train (a diverging lens **L1** transforming the telescope F/11 beam into a F/34.4 beam and a folding mirror **FM1**) that folds the light beam from the telescope into the spectrograph.



**Figure 1.** Simulated Stokes parameters for a solar spectral region assuming an uniform 1 KG magnetic field tilted with respect to the observer line of sight and clockwise rotated of  $45^\circ$  with respect to the equatorial reference system. It has also assumed a projected rotational velocity  $v \sin i = 2 \text{ km s}^{-1}$  (thick continuum) as observed at  $R = 35000$  and  $S/N = 100$  (top-left panel), at  $R = 35000$  and  $S/N = 500$  (top-right panel), at  $R = 115000$  and  $S/N = 100$  (bottom-left panel) and  $R = 115000$  and  $S/N = 500$  (bottom-right panel).

#### 4. THE POLARIMETER

There are several methods to measure the polarisation status of light, all based on intensity measurements at different relative orientation of polarimetric components or at different orientations of the equipment relative to the light source. In a generalised polarimeter, a *Retarder*, with retardance  $\Delta$  and reference axis forming an angle  $\beta$  with respect a reference system, is combined with a *Polariser* whose transmission axis forms an angle  $\alpha$  with the reference system. Clarke & Grainger<sup>4</sup> have shown the advantage of double-beams techniques with respect to single-beam ones, so we discarded *Polariser*, e.g.the Nicol prism, where one of the linearly polarised beam is extinguished.

Two methods are commonly used to perform spectropolarimetry, one is based on a  $\lambda/2$  and a  $\lambda/4$  retarder that can be alternatively inserted along the optical path and rotated with reference to a beam displacer to measure the linear and the circular polarisation respectively. The polarimeters of the AAT (Hough & Bailey<sup>10</sup>) and WHT (Tinbergen & Rutten<sup>14</sup>) are based on this concept. The other method to measure the light polarisation, often called *dual-waveplate* method, is based on a  $\lambda/2$  and a  $\lambda/4$  retarders both inserted along the optical beam. The optical axes of these two retarders are opportunely rotated with respect to a beam displacer to measures the linear and the circular polarisation, as for the William-Wehlau spectropolarimeter (Eversberg et al.<sup>6</sup>).

It has to be noted that both methods need the same number of exposures to measure the linear and the circular polarisation. The advantage of the *dual-waveplate* method is the absence of mechanisms necessary to exchange the retarders, however this method **adds** all the defects of the two retarders and important, for us, it **reduces** the overall efficiency of the polarimeter. Thus we decide not to follow the *dual-waveplate* method.

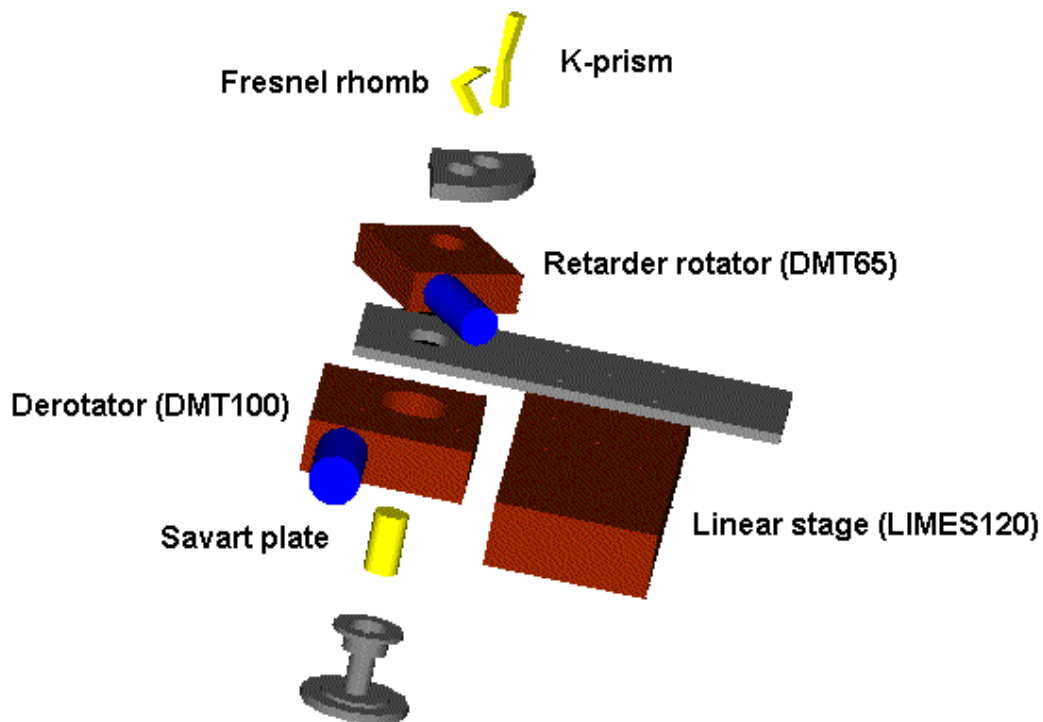


**Figure 2.** Scheme of the polarisation analyser. From the top: the Fresnel rhomb induces a  $\lambda/2$  retardation and the K-prism a  $\lambda/4$  retardation. Mounted on a triangular shaped plate, both retarders can be inserted along the telescope optical beam and rotated with respect to the Savart plate at given angles. The analyser, as a whole, can be continuously rotated, to compensate the sky rotation due to the alto-azimuthal mounting.

To avoid instrumental effects for the TNG, where no Cassegrain focus is present, the ideally location of a polarimeter were just before the tertiary mirror. This solution was not possible both for the high cost of large optical devices and the mechanical difficulties in mounting movable elements before the flat mirror. For the same reasons, it was not possible to locate the polarimeter just after the tertiary mirrors being DOLORES (Device Optimized for the LOw RESolution) permanently installed at the Nasmyth focus. Indeed, as it will be better discussed later, the SARG derotator is itself an optical device changing the polarisation status of light so that it was not possible to include the polarimeter within the spectrograph case.

Designing our polarimeter, we had to overcome three main problems:

- the alto-azimuthal mounting that let the sky be apparently rotating when the polarimetry natural reference system is the equatorial one,
- the instrumental polarisation, changing with the telescope position, due to the two folding mirrors that feed the spectrograph,
- the very large spectral range covered by the SARG.

The polarisation analyser (Fig. 2) is located just on the top of the spectrograph after **L1** and **FM1**. It consists of a  $\lambda/4$  and a  $\lambda/2$  retarder rotating with respect to a beam displacer. The two retarders, simultaneously

available, can be inserted along the telescope optical beam feeding the spectrograph. The axis of the  $\lambda/4$  retarder can form a  $\pm 45^\circ$  angle with respect to the beam displacer optical axis measuring the Stokes V parameter. While the  $\lambda/2$  retarder can assume the 0, 22.5, 45 and  $67.5^\circ$  angles measuring the Stokes Q and U parameters. The polarimeter as a whole can be rotated to compensate the sky rotation due to the alt-azimuthal mounting. The two beams emerging from the beam displacer are subsequently *derotated* by the SARG derotator and appear always aligned with respect to the slit.

The polarimeter is moved in and out the telescope beam by a linear stage.

All optical components were supplied by the *Bernhard Halle Nachfl. GmbH*, Germany.

#### 4.1. Retarders

Because of the very large spectral interval covered by the SARG (370 - 1020 nm), zero and low order retarders were not appropriate. Even achromatic retarders were not suitable being the path-difference correct only in relatively large intervals, i.e. it is within  $\pm 1.5\%$  for the  $\lambda/2$  plate and  $\pm 3\%$  for the  $\lambda/4$  plate only in the spectral range of 430 - 680 nm. As discussed by Goodrich et al.,<sup>7</sup> Pancharatnam superachromatic retarders in principle were acceptable within the covered spectral range. However, Donati et al.<sup>5</sup> reported that super-achromatic wave plates generate ripples. For internal reflections, Fresnel rhombs induce a retard that over a wide range is only minimally wavelength dependent. The difficulty in using Fresnel rhombs to construct a polarimeter is the spatial deviation of the beam that results in a rotating beam when the Fresnel rhomb is rotated (Fig. 4).

Thus, we preferred two optically contacted Fresnel parallelepipeds of BK 7 to rotate the plane of vibration of linearly polarised light (Fig. 4). Differently than the simple Fresnel rhomb, this optical device does not spatially deviate the optical beam so that it can be rotated without experiencing a displacement of the optical beam.

Identically, we adopt a K-prism as  $\lambda/4$  retarder. Fig. ?? shows the prism and the path of rays, together with the phase retardation with wavelengths for the BK7 and suprasil. With the aim to perform spectropolarimetry in the visible range, we chosen the BK7 one. Because of the three reflections within the K-prism the  $\lambda/4$  retarder introduces an image flipping. In our case, we observe a flip of declination when the angle between the retarder and the Savart plate is  $45^\circ$  and a flip in the hour angle when the angle is  $-45^\circ$ . Thus during the exposure sequence, telescope tracking has to be properly settled.

Deviation of  $\pm 0.5$  degrees from the normal incidence change the retardation of  $\pm 0.5\%$  for the Fresnel rhomb and  $\pm 1.7\%$  for the K-prism. Being the focal ratio  $f/34.5$  the average values, weighted by the reflecting ring area of the telescope, are  $\pm 0.17\%$  and  $\pm 0.56\%$  for the Fresnel rhomb for the K-prism respectively.

#### 4.2. Beam displacer

To spatially separate the ordinary and extraordinary beams, we have adopted a Savart plate. This device comprises two beam displacing plates with their optic axes orthogonal. An incident beam propagating through the first plate is resolved into ordinary and extraordinary beams which are displaced from each other in a first principal plane. Upon entering the second plate, the ordinary beam becomes an extraordinary beam, and vice-versa. Displacing again takes place in a second principal plane, which is orthogonal to the first one. The result is two emerging beams displaced along a diagonal. The displacement is  $\sqrt{2}$  times that of each plate. The optical path difference between the two beams is zero, a very important property to have both beams focusing onto the SARG slit.

The separation between the ordinary and extraordinary beams has been fixed at 3 mm to avoid overlapping of orders. Actually, spectropolarimetry is possible with the  $R = 43\,000$  and  $115\,000$  slits. Other available slits are shorter than the Savart plate separation of ordinary and extraordinary beams.

Being the two beams displaced along a direction that forms an angle of  $45^\circ$  with respect to the optical axis of the first calcite plate, all the polarimeter has to be rotated of the same angle to put the two beams on the slit that is oriented in the E-W direction. So that when the  $\lambda/4$  retarder forms a  $45^\circ$  angle with the Savart plate optical axis, we observe a hour-angle flipping and when this angle is  $-45^\circ$  we experience a N-S flipping. Thus during the exposure sequence, auto-guiding can be properly settled just changing the sign of *corrections*. This was the simplest solution we found to avoid writing a new *ad hoc* auto-guiding software for the TNG.

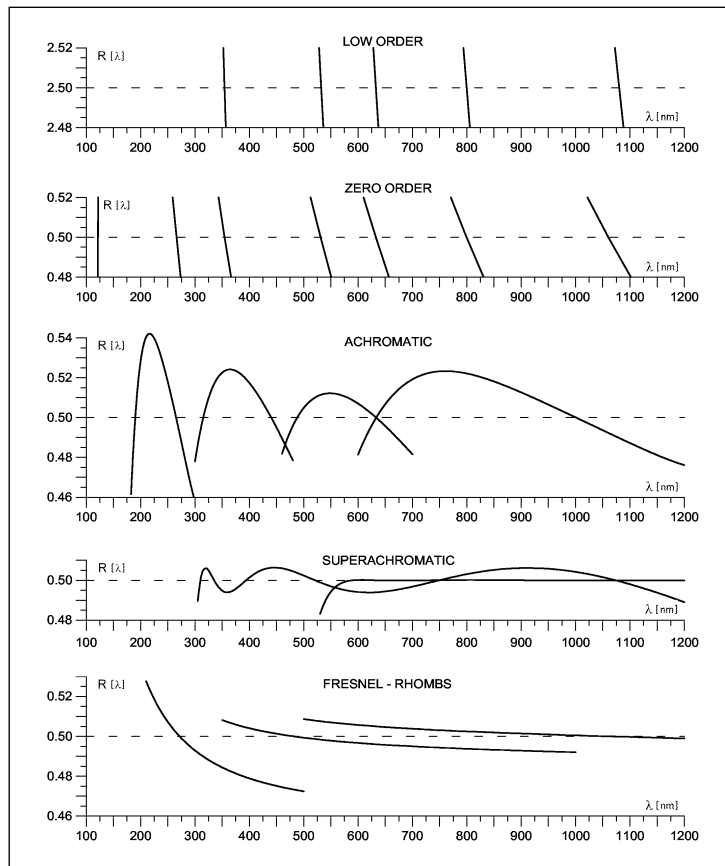


**Figure 3.** Retard induced by different optical devices supplied by the *Bernhard Halle Nachfl. GmbH*. We preferred a BK7 Fresnel rhomb being its retard the closer to that ideal constant value in the whole visible range covered by the SARG spectrograph.

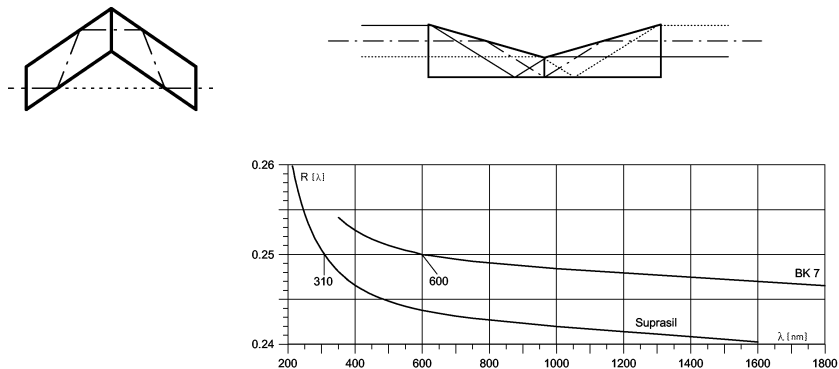


**Figure 4.** Left: Two optically contacted Fresnel parallelepipeds of BK7 are used to induce the  $\lambda/2$  retarder by internal reflection. With respect to a simple Fresnel rhomb, the optical beam is not spatially deviated. Right: K-prism is an optical device inducing a  $\lambda/4$  retarder for internal reflection (top panel). Phase differences as a function of wavelength for the BK7 glass are smaller than for any other retarders.

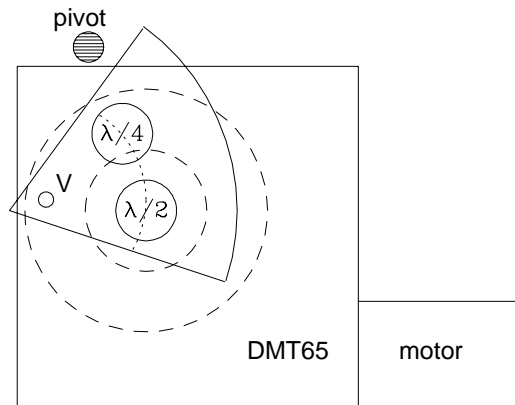


**Figure 5.** A rotary stage is used to rotate the retarders with respect the Savart plate. The central dashed circle defines the hole crossed by the telescope beam. The larger dashed circle defines the rotating ring of the stage where it is fixed for the vertex V a triangular shaped plate. Where the two retarders are mounted with their center located on a circle with center also in V. The triangular plate can rotate around V, so that when it hits the pivot the retarder stops rotating with respect the Savart plate and is moved off from the along the telescope beam. The other retarder is then positioned along the beam.

### 4.3. Mechanics

As it was told in Section 4, to perform spectropolarimetric measurements, retarders have to be rotated with respect to the Savart plate, to have the possibility to perform almost simultaneous linear and circular spectropolarimetry by using **only** one Savart plate, we mount the two retarders on a triangular shaped plate with their centers located on a circle whose center is also a center of rotation for the triangular plate itself (Fig. 5).

The triangular plate is fixed on the rotating ring of a precision rotary stage so that both the retarders can be located in the center of the rotary stage hole that is crossed by the telescope light beam. When a retarder is positioned in the center of the hole of the rotary stage, the optical axis of the retarder can be properly settled with respect to the Savart plate axis just moving the rotary stage that rotates the triangular plate and with it the retarder. Whenever, the rotating triangular plate hits a pivot fixed with respect to the rotary stage, the retarders stops rotating with respect the Savart plate and it is moved off from the telescope beam. The other retarder is then positioned.

Savart plate, DMT65 and retarders are mounted on an further precision rotary stage that compensates the apparent sky rotation due to the alto-azimuthal mounting. The polarimeter is putted in and out of the Telescope beam by means of a precision linear stage.

Positioning precisions are  $0.001^\circ$ ,  $0.002^\circ$  and  $0.0005$  mm for the retarders rotary stage, for the sky derotator and linear stage respectively.

### 4.4. Alignment

To align the optical axis of retarders with respect to the Savart plate optical axis, we have followed Goodrich et al.<sup>7</sup>

To align the retarders with respect to the Savart plate, we simulated the beam telescope and the extraordinary beam emerging from the Savart plate was stopped. A linear polariser was located along the beam between the light source and the Savart plate. The intensity of the emerging beam was then measured as a function of the DMT100 position, and the Savart plate axis was fixed at that angle where the intensity was *null*. Then the

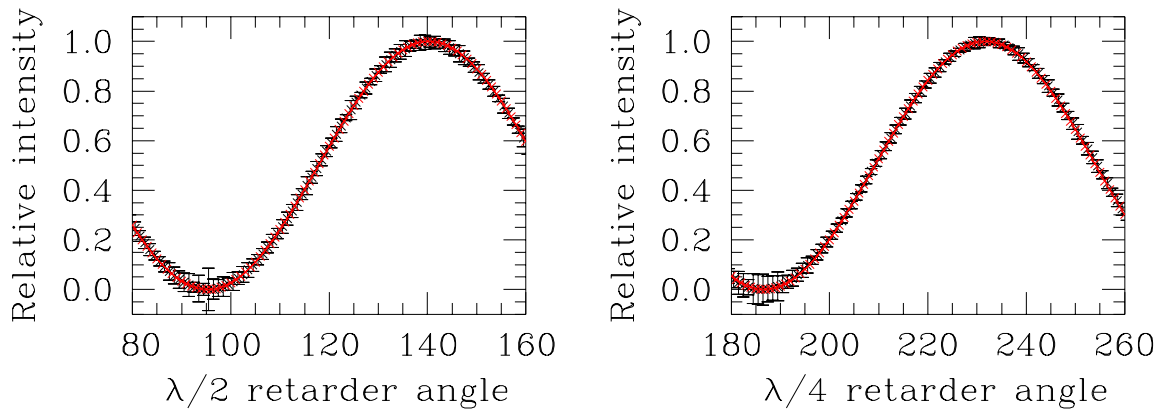


**Figure 6.** Relative intensity of a linearly polarised light emerging as ordinary beam from the Savart plate as a function of the DMT65 angle where retarders are mounted. Data have been recorded at  $1^\circ$  step as the average value of 20 measures, error-bars are two times the standard deviation. Continuum lines are harmonic fits of light variations. As to  $\lambda/4$ , the maximum gives the angle of the rotary stage that puts the retarder be at  $45^\circ$  with respect to the Savart plate. As to  $\lambda/2$ , the maximum gives the angle of the rotary stage that let the optical axis of the retarder aligned with the Savart plate principal axis.

Wavelength (nm)	400	450	500	550	600	650	700	750
Throughput	0.87	0.90	0.90	0.91	0.92	0.92	0.93	0.95

**Table 1.** Throughput of the polarimeter as compared to the SARG..

$\lambda/4$  retarder was inserted after the linear polariser and the beam intensity recorded during the rotation of this retarder performed moving the DMT65. The  $\pm 45^\circ$  angles were fixed determining the maximum intensity of the emerging beam.

Similarly, we have determined the position of  $\lambda/2$  retarder optical axis to be coincident with the beam displacer axis (Fig. 6).

#### 4.5. Depolarising the emerging beams

Beams emerging from the Savart plate are linearly and orthogonally polarised each others and the efficiency of echelle gratings is strongly dependent on the polarisation state of incident light. The *Richardson Lab*, that has supplied the SARG grating, states that the efficiency for the light linearly polarised in the direction of grooves is  $\sim 75\%$  smaller than for light polarised perpendicularly to the grooves.

To avoid different S/N's for the two beams, a  $\lambda/4$  retarder that converts the linear polarised beams in circularly polarised ones should be added. In our case, we do not need further optical components being the SARG derotator itself a K-prism (Gratton et al. 2002).

### 5. THROUGHPUT

To evaluate the throughput of the polarimeter, we have observed some stars without slit. As compared to the SARG alone, the measured efficiency from 400 to 750 nm, is reported in Table 1. It appears that the measured efficiency with wavelength resembles the transmission of BK7.

## 6. MEASUREMENTS OF STOKES PARAMETERS

Following Eversberg et al.<sup>6</sup> and Timbergen & Rutten,<sup>14</sup> the *o*-rdinary and *e*-xtraordinary spectra obtained when the  $\lambda/2$  retarder forms a zero and the  $45^\circ$  angles with respect to the beam splitter optical axis, are related to the Stokes' *Q* parameter by the following relations:

$$\begin{aligned} s_{0,o} &= 0.5 (I + Q)G_o F_0 & s_{45,o} &= 0.5 (I - Q)G_o F_0 \\ s_{0,e} &= 0.5 (I - Q)G_e F_0 & s_{45,e} &= 0.5 (I + Q)G_e F_0 \end{aligned}$$

where *G* is the time independent (instrumental) sensitivity at the given wavelength and *F* is the time dependent sensitivity, as it can be due for example to variation of sky transparency and slit illumination. Hence::

$$\frac{Q}{I} = \frac{R - 1}{R + 1} \quad \text{with} \quad R^2 = \frac{s_{0,o}/s_{0,e}}{s_{45,o}/s_{45,e}}$$

The Stokes' *U* parameter is measured from two exposures obtained when the  $\lambda/2$  retarder forms the  $22.5^\circ$  and  $67.5^\circ$  angles with respect to the beam splitter optical axis from the relation:

$$\frac{U}{I} = \frac{R - 1}{R + 1} \quad \text{with} \quad R^2 = \frac{s_{22.5,o}/s_{22.5,e}}{s_{67.5,o}/s_{67.5,e}}$$

The Stokes' *V* parameter is measured from two exposures obtained when the  $\lambda/4$  retarder forms the  $45^\circ$  and  $-45^\circ$  angles with respect to the beam splitter optical axis from the relation:

$$\frac{V}{I} = \frac{R - 1}{R + 1} \quad \text{with} \quad R^2 = \frac{s_{45,o}/s_{45,e}}{s_{-45,o}/s_{-45,e}}$$

### 6.1. Sky polarisation

From the above relations, it appears for example that:

$$\frac{Q}{I} = \frac{Q_* + Q_{sky}}{I_* + I_{sky}}$$

Hence:

$$\frac{Q_*}{I_*} = \frac{I}{I - I_{sky}} \left( \frac{Q}{I} - \frac{Q_{sky}}{I_{sky}} \frac{I_{sky}}{I} \right)$$

It means that the measured polarisation is coincident with the object polarisation if the sky brightness is negligible with respect to the observed target magnitudes.

Being our analyser to be used with a high resolution spectrograph to measure the polarisation within spectral lines, certainly observed targets are much brighter than the sky even with the full moon.

## 7. INSTRUMENTAL POLARISATION

The SARG is fed by means of the tertiary telescope mirror ( $\mathbf{M}_3$ ) and a further folding mirror ( $\mathbf{FM}_1$ ), so that the instrumental polarisation has to be determined as a function of the target position in the sky. We have removed this polarisation by means of the Muller calculus, considering that: the Stokes parameters describing the polarisation state of the observed target have to be rotated from the equatorial to the alto-azimuthal reference system and than multiplied for the Muller reflection matrix  $R(pa)$  because of the tertiary mirror  $\mathbf{M}_3$  where the polarisation is changed according to the reflection matrix  $T$ . Because of the reflection on second folding mirror  $\mathbf{FM}_1$ , the incidence plane on  $\mathbf{M}_3$  has to be rotated of  $R((\pi/2 - el))$  with *el* elevation angle. Finally being the polarimeter always oriented to the north, we have to perform a further passage from the alto-azimuthal to the equatorial system:

$$IP = R(pa)T(\mathbf{FM}_1)R(\pi/2 - el)T(\mathbf{M}_3)R(pa)$$

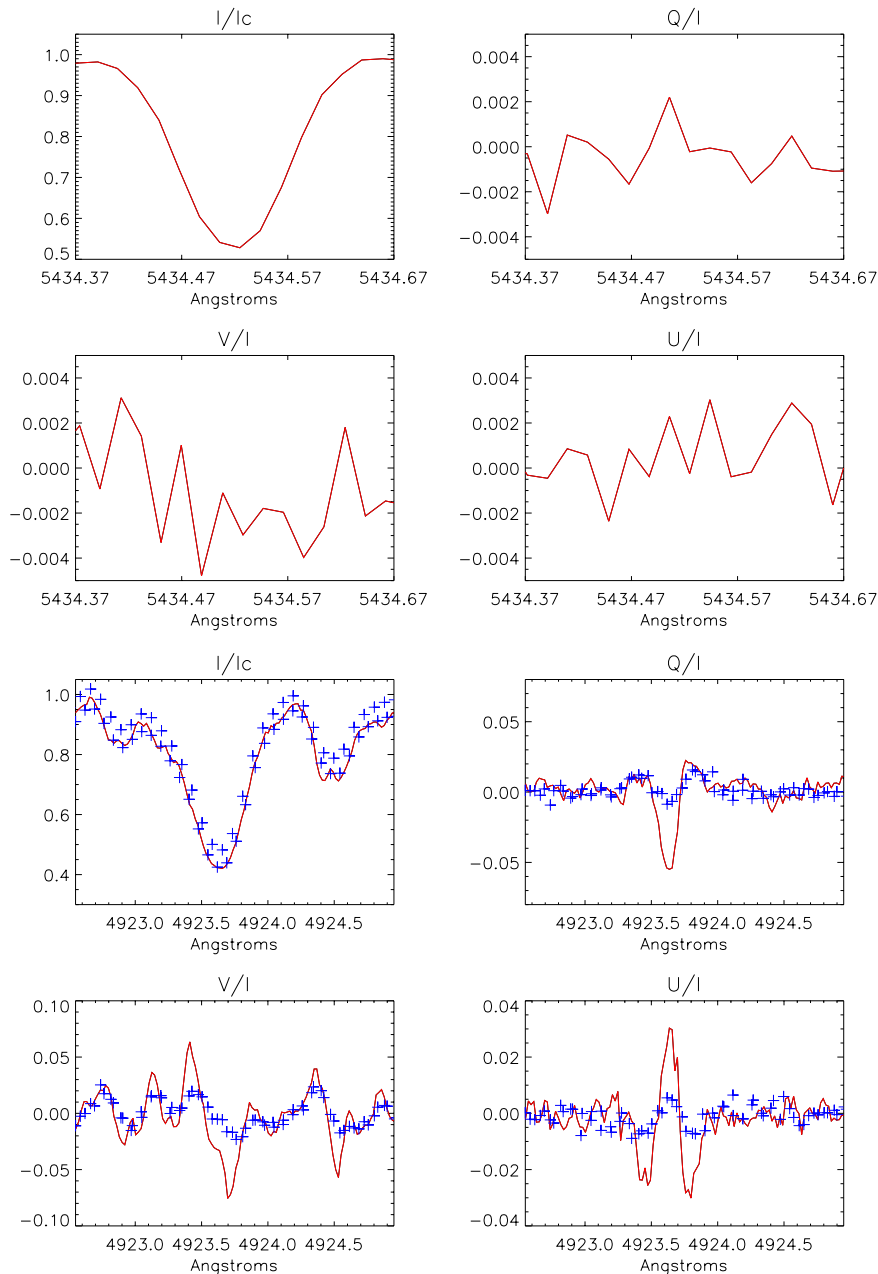


**Figure 7.** Observed polarisation of the Chemically Peculiar star  $\beta CrB$ : Fe I 5434.523 line, that is insensitive to the Zeeman effect because of its null Landé factor and a comparison with MuSiCos spectropolarimetry (crosses) carried out at  $R = 35,000$ .

## 8. POLARISATION ACROSS SPECTRAL LINES

Fig. 7 shows our results for the Magnetic Chemically Peculiar star  $\beta CrB$  ( $V = 3.7$ ) observed at  $R = 115,000$  with six exposures of 360 seconds. The case of Fe5435 Å line, with null Landé factor and then without intrinsic polarisation, shows the correct handling of the instrumental polarisation and reduction procedures. The 4922 Å region shows the advantage of our high resolution ( $R = 115,000$ ) when compared with observations with a larger smearing function ( $R = 35,000$ ).

## REFERENCES

1. Babcock, H.W., 1947, *ApJ* 105, 105
2. Bortoletto, F., Bonoli, C., D'Alessandro, M., Ragazzoni, R., Conconi, P., Mancini, D., Pucillo M. 1998, in *Astronomical telescopes and Instrumentation*, SPIE, 3352, 91
3. Capitani, C., Cavallini, F., Ceppatelli, G., Landi degl'Innocenti E., Landi degl'Innocenti M., Landolfi, M., Righini, A., 1989, *Solar Physics* 120, 173
4. Clarke, D., Grainger, J.F. 1971, *Polarized light and optical measurement*, Pergamon Press
5. Donati, J.-F., Catala, C., Wade, G.A., Gallou, G. & Delaigue, G., Rabou, P. 1999, *A&AS* 134, 149
6. Eversberg, T. Moffat, A.F.J., Debruyne, M., Rice, J.B., Piskunov, N, Bastien, P., Wehlau, W.H., Chesneau, O. 1998, *PASP* 110, 1356
7. Goodrich, R.W., Cohen, M.H., Putney, A. 1995, *PASP* 107, 179
8. Gratton, R. Bonanno, G., Bruno, P., Calì, A., Claudi, R., Cosentino, R., Desidera S., Diego, F., Farisato, G., Martorana, G., Rebeschini, M., Scuderi, S. 2002, *Instrumental Astronomy* (in press)
9. Harries, T. J., Howarth, I. D. 2002, *A&A* 361, 139
10. Hough, J., Bailey, J. 1994, in *Spectropolarimetry at the AAT* (The AAT User's manual 24.2)
11. Kawabata, K. S., Akitaya, H., Hirakata, N., Hirata, R., Ikeda, Y., Isogai, M., Karube, T., Kondoh, M., Matsumura, M., Nakayama, S., Okazaki, A., Seki, M. 2001, *ApJ* 552, 782
12. Schmid, H. M., Appenzeller, I., Camenzind, M., Dietrich, M., Heidt, J., Schild, H. & Wagner, S. 2001 *A&A* 372, 59
13. Solanki, S.K., Stenflo J.O. 1986, *A&A* 170, 120
14. Tinbergen, J., Rutten, R. 2000, in *Measuring polarization with ISIS users' manual*. The Isaac Newton Group of Telescopes.